JOURNAL OF VIROLOGY, Sept. 1996, p. 6216–6226 Vol. 70, No. 9
0022-538X/96/$04.00+0

Identification of Latent Membrane Protein 2A (LMP2A) Domains Essential for the LMP2A Dominant-Negative Effect on B-Lymphocyte Surface Immunoglobulin Signal Transduction

SARA FRUEHLING,[1] SUK KYEONG LEE,[1] RUTH HERROLD,[1] BARBARA FRECH,[2] GERHARD LAUX,[3] ELISABETH KREMMER,[4] FRIEDRICH A. GRÄSSER,[2] AND RICHARD LONGNECKER[1]*

Department of Microbiology–Immunology, Northwestern University Medical School, Chicago, Illinois,[1] and Abteilung Virologie, Institut für Medizinische Mikrobiologie und Hygiene, Universitätskliniken des Saarlandes, D-66421 Homburg/Saar,[2] GSF, Institut für Klinische Molekularbiologie und Tumorgenetik im Forschungszentrum für Umwelt und Gesundheit,[3] and GSF, Institut für Immunologie,[4] D-81377 München, Germany

Received 1 May 1996/Accepted 7 June 1996

Epstein-Barr virus (EBV) recombinants which carry three different deletion mutations in the LMP2A cytoplasmic amino-terminal domain were constructed. The presence of each mutation, LMP2AΔ21-36, LMP2AΔ21-64, and LMP2AΔ21-85, in EBV-infected transformed lymphoblastoid cell lines was confirmed by PCR analysis and Southern blot hybridization. Confirmation of mutant LMP2A protein expression was by immunofluorescence and immunoblotting with a newly identified rat monoclonal antibody that recognizes each of the LMP2A deletion mutations. Lymphoblastoid cell lines infected with recombinant EBV DNAs containing the mutations were analyzed for loss of LMP2A's dominant-negative effect on surface immunoglobulin signal transduction by monitoring induction of tyrosine phosphorylation, calcium mobilization, and activation of lytic replication following surface immunoglobulin cross-linking. Domains of LMP2A important for induction of tyrosine phosphorylation, calcium mobilization, and activation of lytic replication were identified.

Epstein-Barr virus (EBV) is a human herpesvirus and is the causative agent of mononucleosis in healthy adolescents and causes a lymphoproliferative disease in immunocompromised humans, marmosets, and SCID mice (11, 12, 31). EBV is a factor associated with African Burkitt's lymphoma, Hodgkin's disease, nasopharyngeal carcinoma, and oral hairy leukoplakia (11, 12, 31). EBV latently infects B lymphocytes in vitro and in vivo. In vitro latent infection is characterized by expression of EBV nuclear antigens (EBNA1, EBNA2, EBNA3A, EBNA3B, EBNA3C, and EBNALP), and latent membrane proteins (LMP1, LMP2A, and LMP2B) (11, 12, 31). LMP2A and LMP2B are also known as terminal proteins 1 and 2 (TP1 and TP2) (16, 17, 38). The LMP2 message is consistently detected in nasopharyngeal carcinoma tumor biopsies and EBV malignancies and, along with EBNA1, is the only EBV-specific message detected in individuals harboring EBV latent infections (36, 46), suggesting that LMP2 may play an important role in vivo for viral replication, persistence, and EBV-related diseases in humans.

LMP2 is transcribed by two different promoters 3 kb apart (16, 17, 39). The first exons of LMP2A and LMP2B are the only unique exons, and the remaining eight exons are common to both messages (16, 17, 39). The first LMP2A exon encodes a 119-amino-acid cytoplasmic domain, while the first LMP2B exon is noncoding (Fig. 1A). The methionine at amino acid 120 of LMP2A is the first methionine in the first LMP2 common exon and is the initiation site for LMP2B. LMP2A and LMP2B share 12 hydrophobic transmembrane domains and a 27-amino-acid cytoplasmic carboxyl-terminal domain (Fig. 1A). LMP2A and LMP2B form aggregates in the plasma membranes of B lymphocytes (20). The LMP2A cytoplasmic amino-terminal domain associates with Src family protein tyrosine kinases (PTKs) (2) and the Syk PTK (28). LMP2A expression in EBV-negative B-lymphoma cells prevents normal calcium mobilization which follows surface immunoglobulin (sIg) cross-linking (30).

Previous mutational analysis of LMP2 reveals that neither LMP2A nor LMP2B is essential for in vitro infection or transformation of primary B lymphocytes (13, 22–24). Analysis of lymphoblastoid cell lines (LCLs) infected with LMP2 mutants has specified a role of LMP2A in maintaining EBV latency in EBV-infected LCLs. The 119-amino-acid cytoplasmic amino-terminal domain, unique to LMP2A, is essential for the function of LMP2. EBV^+ $LMP2A^+$ LCLs are blocked in sIg-stimulated calcium mobilization, tyrosine phosphorylation, and lytic activation (Fig. 1B) compared with EBV^+ $LMP2A^-$ LCLs (28, 29). LMP2A functions as a negative regulator of the Src family Lyn PTK and the Syk PTK (28), while LMP2B may regulate LMP2A function by modulating spacing between individual LMP2A amino-terminal domains in LMP2A aggregates in the plasma membranes of EBV^+ $LMP2A^+$ LCLs (21).

The amino-terminal domain of LMP2A contains tyrosine residues which are phosphorylated both in EBV^+ $LMP2A^+$ LCLs and in LMP2A transfectants (2, 19, 28). Most of the phosphotyrosine reactivity in latently infected B lymphocytes is associated with LMP2A patches (2, 19, 28). Constitutively clustered membrane patches of tyrosine-phosphorylated LMP2A might mimic activated receptor complexes, thereby competing for proteins with *src* homology 2 (SH2) domains. SH2 domains are noncatalytic domains conserved among cytoplasmic signaling proteins which bind tyrosine-phosphorylated proteins (34, 35). Recent studies have shown that sequences adjacent to the tyrosine residues confer preference for binding a particular SH2 domain. Different SH2 domains have differing preferences for hydrophobic or hydrophilic residues immediately adjacent to a tyrosine residue (40, 41). Comparing the eight tyrosine residues of LMP2A and their surrounding motifs re-

* Corresponding author. Mailing address: Department of Microbiology–Immunology, Northwestern University Medical School, 303 E. Chicago Ave., Chicago, IL. Phone: (312) 503-0467. Fax: (312) 503-1339. Electronic mail address: r-longnecker@nwu.edu.

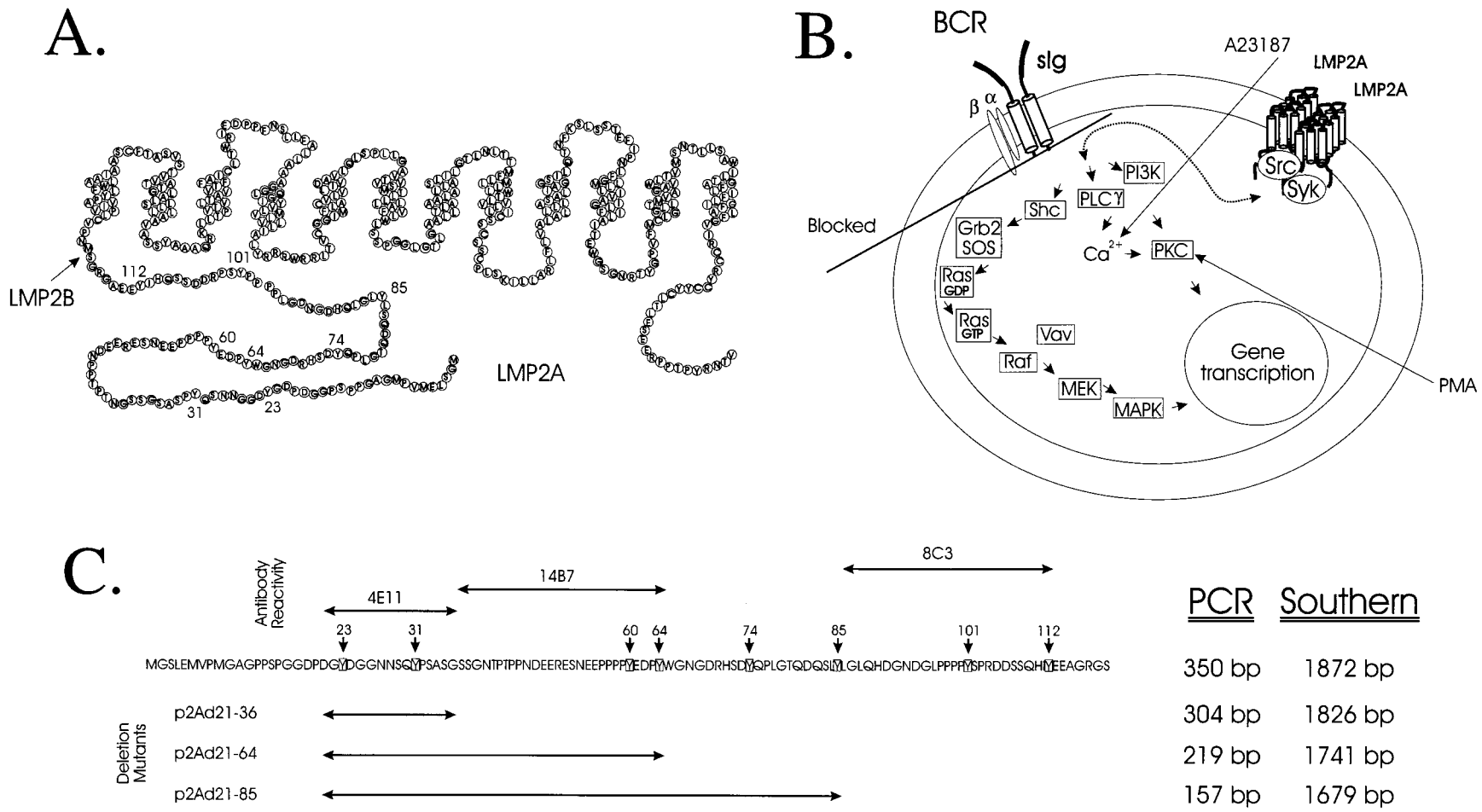

FIG. 1. (A) Schematic of the predicted structure of LMP2 in a B-lymphocyte plasma membrane. LMP2A and LMP2B both contain 12 hydrophobic transmembrane domains and a 27-amino-acid cytoplasmic carboxyl-terminal domain. LMP2B initiates at the methionine, indicated by the arrow, and does not contain the 119-amino-acid cytoplasmic amino-terminal domain unique to LMP2A. Numbers denote the locations of the 8 tyrosine residues in LMP2A's amino-terminal domain. (B) LMP2A in a plasma membrane of EBV-infected B lymphocytes blocks normal B-cell receptor (BCR) signaling pathways and blocks cellular and viral gene transcription. LMP2A aggregates in the plasma membrane and associates with the Src family PTKs and the Syk PTK. LMP2A's effect most likely occurs at the plasma membrane, since wild-type-infected LCLs can be transcriptionally activated, bypassing the LMP2A block by exposure to calcium ionophores or phorbol esters. PI3K, PI(3)kinase; PKC, protein kinase C; PMA, phorbol myristate acetate; MEK, MAP-ERK kinase; MAPK, mitogen-activated protein kinase. (C) Amino acid sequence of the LMP2A amino-terminal domain with the 8 tyrosine residues indicated. To investigate the potential role of the first six tyrosine residues in LMP2A's ability to block normal B-cell signaling events, LCLs with three deletion mutations within LMP2A's amino-terminal domain were generated. The deletions eliminated a total of 16, 44, and 65 amino acids, including 2, 4, and 6 tyrosine residues, respectively. The incorporation of each LMP2A deletion into recombinant virus was identified by PCR and verified by Southern blot hybridization. The sizes of both the wild-type and mutant LMP2A products by both analyses are indicated. The regions of LMP2A required for recognition by the three rat monoclonal antibodies (4E11, 14B7, and 8C3) are indicated by arrows above the LMP2A sequence.

veals homology to several motifs which predict optimal binding to identified proteins involved in signal transduction. The LMP2A tyrosine 31 (Y-31) motif (YPSA) has homology with group III tyrosine motif members, which are defined by a Y-hydrophobic–X-hydrophobic sequence (40, 41). This phosphotyrosine motif optimally binds the SH2 domain of proteins like the 85-kDa subunit adapter proteins of PI(3)kinase, PLC2γ, and Shc. LMP2A Y-60 (YEDP) contains the general Y-hydrophilic–hydrophilic-I or -P motif or the group IB motif. Of the group IB proteins, Y-60 has the best homology with the Nck (YDEP) motif. LMP2A Y-74 and Y-85 are homologous to a common cytoplasmic motif which couples intracellular PTKs with lymphocyte antigen receptors. The minimal functional motif, first described by Reth (37) and recently designated the immuno-receptor tyrosine-based activation motif (ITAM), consists of paired tyrosines and leucines (4). ITAMs are important for binding and subsequent activation of SH2-containing proteins following sIg receptor stimulation (1, 5, 48). It is likely the Syk SH2 domains interact with LMP2A via Y-74 and Y-85 (28). The Y-101 motif (YSPA) contains an unusual arginine at the +3 position which is characteristic of the Csk SH2 preferred motif. The Y-112 phosphotyrosine motif (YEEA) is clearly similar to the Src family PTK SH2 binding motif (YEEI). Lastly, LMP2A Y-23 and Y-64 contain phosphotyrosine motifs that have no predicted specificity to any identified SH2 domain.

To further delineate the region(s) of the amino-terminal domain of LMP2A required for LMP2A-negative regulation of sIg signal transduction, three LMP2A deletions were constructed and recombined into the EBV genome. The primary focus was on the first six tyrosine residues and their potential importance in the LMP2A-mediated block in sIg signal transduction. LMP2A amino acids 21 to 36, 21 to 64, and 21 to 85 were deleted, removing two, four, or six of the tyrosines contained within the LMP2A amino-terminal cytoplasmic domain. LCLs infected with each mutation, as well as wild-type controls, were tested for calcium mobilization, tyrosine phosphorylation, and activation of lytic replication following sIg cross-linking.

MATERIALS AND METHODS

Cell lines and cell culture. All cell lines were maintained in RPMI 1640 medium containing 10% inactivated fetal bovine serum, 1,000 U of penicillin per ml, and 1,000 μg of streptomycin (Sigma) per ml. BJAB is an EBV-negative B-lymphoma cell line (26). The HH514-16 subclone of the original EBV-infected P3HR1 (P3JHR1) Burkitt's lymphoma cell line (a gift of George Miller) has EBV genomes with only a single type of DNA, from which the segment encoding EBNA2 and the last two exons of EBNALP are deleted (10). B95-8 is an EBV-infected marmoset cell line that is partially permissive for viral replication (32, 33). WT1 and WT4 are EBV^+ $LMP2A^+$ LCLs, and ES1 and ES4 are EBV^+ $LMP2A^-$ LCLs (29). Primary human mononuclear cells were obtained from blood samples of healthy donors by centrifugation over a cushion of Ficoll-Paque (Pharmacia). For EBV-positive donors, T lymphocytes were removed as previously described (25).

Construction of plasmids. pSVNaeZ, used to induce lytic EBV replication, and *Eco*RI-A, used to rescue the EBNA2 and EBNALP mutations contained in the P3HR1 cell line, have been described previously (25, 44). Amino acids 21 to 36, 21 to 64, and 21 to 85 (Fig. 1) of LMP2A were deleted by a PCR-based strategy from genomic and cDNA constructs. Genomic mutations were incorporated into pRH6, which contains a *Kpn*I (B95-8 bp 161,097)-to-*Eco*RI (B95-8 bp 1) fragment from B95-8 EBV DNA. cDNA mutations were incorporated into pLMP2A (19). All mutants were sequenced to confirm the presence of the desired mutation and the absence of any mutations introduced by PCR. Other cDNA LMP2A deletion mutations have been previously described (19).

Transfection. DNA used for transfections was banded twice on CsCl density gradients. BJAB cells were electroporated as previously described (19). Recombinant cell lines were generated by transfecting 10^7 P3HR1 cells in 0.4 ml of complete RPMI 1640 medium with 15 μg of pSVNaeZ, 7 μg of *Eco*RI-A, and 25 μg of recombinant LMP2A DNA. Cells were pulsed once at 200 V with a Gene Pulser (Bio-Rad) with a 960-μF capacitance in a 0.4-cm-electrode-gap cuvette (Bio-Rad) and immediately diluted in 10 ml of complete RPMI 1640 medium. The induction of lytic EBV replication in LCLs was performed similarly, except these cells were pulsed at 230 V with 25 μg of pSVNaeZ and diluted in complete RPMI 1640 medium containing 20 ng of 12-*O*-tetradecanoylphorbol-13-acetate per ml.

Infection of primary cells. The recombinant virus, generated from transfected P3RH1 cells, was freed from host cells by freeze-thawing, sonication, and filtration through a 0.45-μm-pore-size filter. This cell-free viral supernatant was used to infect primary blood mononuclear cells or purified B lymphocytes in culture. Cells were infected by incubating 7×10^6 cells with 2 ml of virus or virus diluted 1:10 for 1 h at 37°C. Infected cells were pelleted and resuspended in 15 ml of complete RPMI 1640 medium, and 7×10^4 cells were plated in 0.15-ml aliquots per well of a 96-well culture plate. Infected cells were fed with 0.1 ml of complete RPMI 1640 medium 14 days after plating. LCLs emerged 3 to 5 weeks after initial plating, and screening of LCLs containing the LMP2A deletions began at 6 to 8 weeks. Expression of sIg was determined by flow cytometry with a fluorescein isothiocyanate-linked goat anti-human Ig (H+L; Southern Biotech) diluted 1:50 as previously described (30).

PCR analysis. Genomic DNA from LCLs was prepared (44) and amplified in a 25-μl volume for 40 cycles as previously described (22). Primers 5′LMP2A (CTGCTGCAGCTATGGGGTCC) and 3′LMP2A (GCATATACACAACTCT ACTCAGTAGGG) specific for the sites of the deletions were used to screen for the presence of a mutation. The p2AΔ21-36 construct contained a 46-nucleotide deletion, the p2AΔ21-64 construct contained a 131-nucleotide deletion, and the p2AΔ21-85 construct contained a 193-nucleotide deletion. The expected amplified PCR products were 304, 219, and 157 bp, respectively. Ethidium bromide-stained PCR products were viewed after electrophoresis through 4% Metaphor agarose (FMC Bioproducts).

Southern blot hybridization. A 1,872-bp fragment, generated from a *Bgl*I digest of pRL49 (22) was isolated and utilized as a ^{32}P-labeled probe for Southern blot hybridization. Genomic DNA was prepared by cell lysis, proteinase K treatment, phenol extraction, and ethanol precipitation (47). Prepared DNAs from representative LCLs were digested with *Bgl*I, separated by electrophoresis on a 1% agarose gel, transferred to a nylon membrane (GeneScreen), and probed as previously described (47).

LMP2 rat monoclonal antibodies. Rat monoclonal antibodies specific for LMP2 were generated by following the general procedure previously described (15). Briefly, Lou/C rats were immunized with a bacterial trpE-LMP2A fusion protein (9) with the pATH10 vector described previously (14), which contains the B95-8 LMP2A open reading frame. Monoclonal antibodies, reacting with trpE-LMP2A but not the parental trpE nonfusion protein, were identified by enzyme-linked immunosorbent assay and confirmed by immunofluorescence and immunoblot analysis with a baculovirus-expressed LMP2A protein (8). The subclasses of three selected clones, 8C3 (IgG1), 4E11 (IgG1), and 14B7 (IgG2a), were determined with mouse-anti-rat subclass-specific antibodies (42). Finally, the antibodies were tested by immunoblot analysis with 12-*O*-tetradecanoylphorbol-13-acetate-stimulated B95-8 cell extracts.

Immunoprecipitation of radiolabeled cells. BJAB cells (10^7 cells per immunoprecipitation) were transfected with 50 μg of pLMP2A or vector alone (pSG5) and labeled with [^{35}S]methionine as described previously (19). Ten hours after transfection, cells were washed in phosphate-buffered saline (PBS) and lysed in 1% NP-40 lysis buffer (1% Nonidet P-40, 50 mM Tris-HCl [pH 7.4], 150 mM NaCl, 2 mM EDTA, 10 μg [each] pepstatin and leupeptin per ml, 0.5 mM phenylmethylsulfonyl fluoride, 1 mM sodium orthovanadate) and the insoluble material was removed by centrifugation at 4°C. Cleared lysates were immunoprecipitated with each of the three rat monoclonal antibodies or a rabbit polyclonal antiserum (50 μl per immunoprecipitation) (20) for 1 h at 4°C, captured with protein G or A Sepharose, respectively, washed four times in 1% NP-40 lysis buffer, mixed with equal volumes of 2× sodium dodecyl sulfate (SDS) sample buffer, incubated at 95°C for 1 min, and separated by SDS–8% polyacrylamide gel electrophoresis (PAGE). Proteins were transferred to nitrocellulose (Scheicher & Schuell) and subjected to autoradiography.

Immunoblotting. (i) LMP2A. LCLs or transfected BJAB cells (10^7 cells) were washed twice in PBS and lysed in 1% NP-40 lysis buffer, and the insoluble material was removed by centrifugation at 4°C. Lysates were heated at 70°C for 5 min, separated by SDS–8% PAGE, transferred to nitrocellulose, blocked with 4% milk for 1 h at room temperature (RT), probed with a 1:50 dilution of the rat monoclonal antibodies directed against LMP2A for 1 h at RT, washed with Tris-buffered saline-Tween (TBST), incubated with horseradish peroxidase (HRP)-linked anti-rat secondary antibody (Amersham) diluted 1:300 for 30 min at RT, and detected by enhanced chemiluminescence (ECL) (Amersham).

(ii) Phosphotyrosine. Cellular activation and preparation of lysates were performed as previously described (28). In brief, 6×10^7 cells were resuspended and equilibrated in serum-free RPMI medium for 15 min at 37°C. Cells were stimulated with 25 μg of goat anti-human Ig (Southern Biotechnology) per ml for the indicated times, and cells were immediately lysed in 1% NP-40 lysis buffer. The insoluble material was removed by centrifugation at 4°C, and cleared supernatants were immunoprecipitated for 1 h at 4°C with PY20 (Transduction Laboratories) and captured with protein A-Sepharose (Sigma). Captured lysates were washed four times with 1% NP-40 lysis buffer and separated by electrophoresis through an SDS–8% polyacrylamide gel. Proteins were transferred to nitrocellulose, blocked in 5% bovine serum albumin (BSA)–1% milk, incubated with

PY20-HRP (Santa Cruz) for 30 min at RT, washed in TBST, and detected by ECL (Pierce).

(iii) BZLF1. LCLs (4×10^6 cells) were either treated with 100 μg of goat anti-human IgF(ab′)$_2$ (Jackson Immuno Laboratories) per ml or left untreated for 48 h at 37°C. After incubation, cells were washed in PBS and whole-cell lysates were separated by electrophoresis through an SDS–8% polyacrylamide gel. Proteins were transferred to nitrocellulose, blocked in 5% milk, incubated with BZ1 monoclonal antibody to the BZLF1 protein (49) or with a human serum reactive to EBV lytic antigens for 1 h at RT (29), incubated with a secondary anti-mouse-HRP antibody or protein A-HRP, washed in TBST, and detected by ECL (Pierce).

Immunofluorescence. Immunofluorescence of LCLs was performed as previously described (20). In brief, LCLs were fixed to glass slides with acetone at −20°C for 5 min, blocked with 20% normal goat serum for 10 min at RT, incubated with rat monoclonal antibody (8C3) diluted 1:50 for 1 h, and then incubated with an anti-rat tetramethyl rhodamine isothiocyanate secondary antibody diluted 1:1,000 (Jackson Laboratory), washed in PBS, and viewed with a Zeiss fluorescence Axioscope.

Calcium mobilization. Tissue culture cells (3×10^6 cells) were resuspended in loading buffer (145 mM NaCl, 5 mM KCl, 1 mM $MgCl_2$, 1 mM $CaCl_2$, 10 mM glucose, 10 mM HEPES [*N*-2-hydroxyethylpiperazine-*N*′-2-ethanesulfonic acid], 1% BSA, 2.5 mM probenecid) and loaded with a 2 mM calcium-binding dye, fluo-3-acetoxymethyl ester (fluo-3) (Molecular Probes) for 30 min at RT. After loading, the cells were washed twice and resuspended in loading buffer. The prepared cells were then measured for fluorescence after sIg cross-linking in a Perkin-Elmer LS-5B luminescence spectrometer. Excitation and emission values for fluo-3 are 505 and 530 nm, respectively. The Autofluorescence (or minimal fluorescence) value for each LCL was also determined by performing the above procedure without adding fluo-3 dye. Baseline fluorescence was recorded for 1 min, and maximal fluorescence was measured after addition of digitonin (40 μM). Calcium concentration (in nanomolar units) was calculated according to the formula $Ca^{2+} = 400(F - \text{Fmin})/(\text{Fmax} - F)$, where F is baseline fluorescence, Fmin is minimal fluorescence, and Fmax is maximal fluorescence (18, 27).

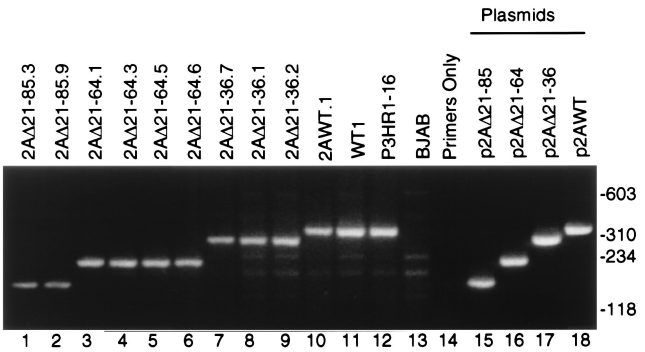

FIG. 2. PCR analysis of wild-type and LMP2A mutant EBV-infected LCLs. LCL DNA was prepared by cell lysis and proteinase K treatment. Prepared DNA was amplified 40 cycles with primers 5′LMP2A and 3′LMP2A, which amplify the first 350 nucleotides of LMP2A. The ethidium bromide-stained PCR products were viewed after electrophoresis through 4% Metaphor agarose. LCLs infected with wild-type virus (lanes 10 to 12) contain the expected wild-type LMP2A product of 350 bp, while representative LCLs infected with the LMP2A deletion mutants show the expected decrease in size of the LMP2A-amplified products. Amplified products of 304 bp for LMP2AΔ21-36 LCLs (lanes 7 to 9), 219 bp for LMP2AΔ21-64 LCLs (lanes 3 to 6), and 157 bp for LMP2AΔ21 to 85 LCLs (lanes 1 and 2), which agree with the expected values shown in Fig. 1C, were detected. Both the parental and LMP2A deletion mutant plasmids were subjected to PCR and were run simultaneously to verify the sizes of the amplified products (lanes 15 to 18). Marker DNA is shown in base pairs at the right.

RESULTS

Construction of LCLs infected with recombinant EBV containing deletion mutations in LMP2A. PCR-mediated mutagenesis was used to create EBV DNA fragments encoding each of the three LMP2A deletion constructs depicted in Fig. 1C. The smallest deletion, LMP2AΔ21-36, lacked 16 amino acids, including LMP2A's first two tyrosine residues; the middle deletion, LMP2AΔ21-64, lacked 44 amino acids, including the first four tyrosine residues; and the largest deletion, LMP2AΔ21-85, lacked 65 amino acids, including the first six tyrosine residues and the LMP2A ITAM motif. These recombinant LMP2A constructs were verified by sequencing and then incorporated into virus through a strategy utilizing the transformation-incompetent, replication-competent EBV deletion mutant, P3HR1. Recombinant virus was generated by the cotransfection of the P3HR1 cell line with pSVNaeZ DNA to induce lytic viral replication, with *Eco*RI-A DNA to rescue the EBNA2 and EBNALP deletions in the P3HR1 cell line, and with each of the recombinant LMP2A DNA fragments (22). P3HR1 genomes that restored the EBNA2 and EBNALP deletions through a homologous recombination event may also have incorporated the LMP2A mutation through a similar recombination event. The recombinant virus generated in this procedure was freed from cells by freeze-thawing, sonication, and filtration. This cell-free viral supernatant was used at two dilutions to infect primary B lymphocytes in culture.

Identification of EBV$^+$ LMP2A deletion mutant LCLs. Four to six weeks after the initial infection, transformed cells were identified and analyzed by PCR for virus incorporating the desired LMP2A mutation. Primers that amplified the first 350 bp of LMP2A were utilized, and mutant virus was identified by the smaller amplified LMP2A product. Amplifications using DNA prepared from LCLs with wild-type LMP2A contained the expected wild-type product of 350 bp (Fig. 2, lanes 10 to 12). Representative LCLs for each of the LMP2A deletion mutants also contained, as expected, a smaller amplified product. LMP2AΔ21-36-representative LCLs (Fig. 2, lanes 7 to 9) appeared to be 304 bp in length; LMP2AΔ21-64 LCLs (Fig. 2, lanes 3 to 6) appeared to be 219 bp in length; and LMP2AΔ21-85 LCLs (Fig. 2, lanes 1 and 2) appeared to be 157 bp in length. Expected sizes of amplified products are illustrated in Fig. 1C. Plasmids used to make the LMP2A mutations were amplified and run simultaneously to verify the sizes of the amplified products (Fig. 2, lanes 15 to 18).

To verify correct incorporation of LMP2A deletion constructs within the generated LCLs, Southern blot hybridization was performed (Fig. 3). Genomic DNAs from representative EBV$^+$ LMP2A$^+$ and EBV$^+$ LMP2A deletion mutant LCLs were digested with *Bgl*I and probed with a 1,872-bp *Bgl*I LMP2A DNA fragment. As expected, the wild-type 1,872-bp fragment was present in both the B95-8 cell line and the representative EBV$^+$ LMP2A$^+$-infected LCL (Fig. 3, lanes 1 and 3). In representative EBV$^+$ LMP2A deletion mutant LCLs, a 1,826-bp fragment (LMP2AΔ21-36 LCL [Fig. 3, lane 4]), a 1,741-bp fragment (LMP2AΔ21-64 LCLs [lanes 5 to 8]), and a 1,679-bp fragment (LMP2AΔ21-85 LCLs [lanes 9 to 10]) were readily detected as expected. The wild-type *Bgl*I fragment was not detected in any of the EBV$^+$ LMP2A deletion mutant LCLs even upon prolonged exposure of the blot, indicating that the LMP2A wild-type allele had been replaced with the LMP2A mutant allele in the EBV$^+$ LMP2A deletion mutant LCLs.

Identification of LMP2-specific rat monoclonal antibodies. A bacterial TrpE-LMP2A fusion protein (8) was used to immunize Lou/C rats as described previously (15). Fusion of the myeloma cell line P3X63 Ag 8.653 with rat immune spleen cells and screening of hybridoma supernatants were done as previously described (15). Three hybridomas (8C3, 14B7, and 4E11) which reacted with the TrpE-LMP2A fusion protein but not with TrpE alone (data not shown) were identified.

Antibody specificities of the three hybridoma supernatants were evaluated by transfecting BJAB cells with LMP2A (pLMP2A) or control (pSG5) cDNA expression vectors. Following transfection, cells were incubated in [^{35}S]methionine for 10 h and lysed in nonionic detergent. Immunoprecipita-

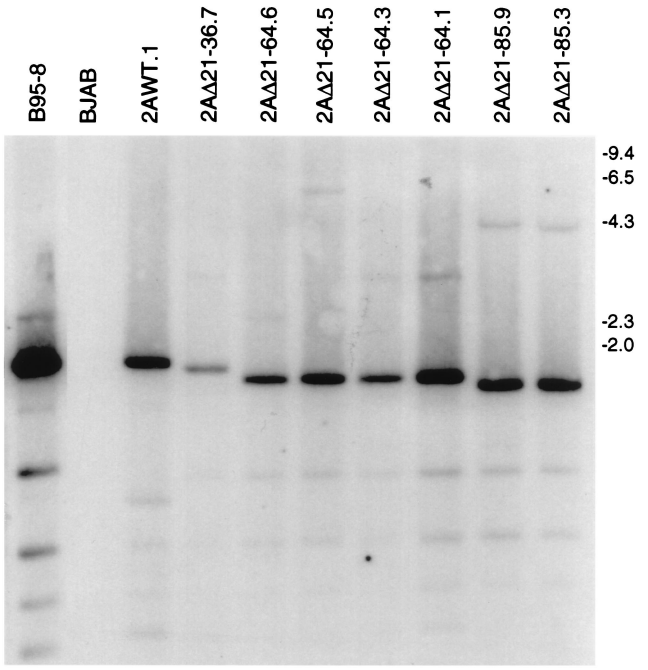

FIG. 3. Southern blot hybridization of wild-type and mutant LMP2A-expressing LCLs. LCL DNA was prepared by cell lysis, proteinase K treatment, phenol extraction, and ethanol precipitation. Prepared DNAs from representative LCLs were digested with *Bgl*I, run out on a 1% agarose gel, transferred to a nylon membrane, and probed with a ^{32}P-labeled 1,872-bp *Bgl*I fragment. Two LCLs containing wild-type LMP2A (lanes 1 and 3) demonstrate the expected 1,872-bp wild-type size. LCLs incorporating the LMP2A deletions LMP2AΔ21-36, -Δ21-64, and -Δ21-85 appear to be 1,826 bp (lane 4), 1,741 bp (lanes 5 to 8), and 1,679 bp (lanes 9 to 10), respectively. The absence of the wild-type-sized fragment with any of the mutant LCLs indicates that these LCLs contain only mutant alleles of LMP2A. Lambda markers are shown in kilobases at the right.

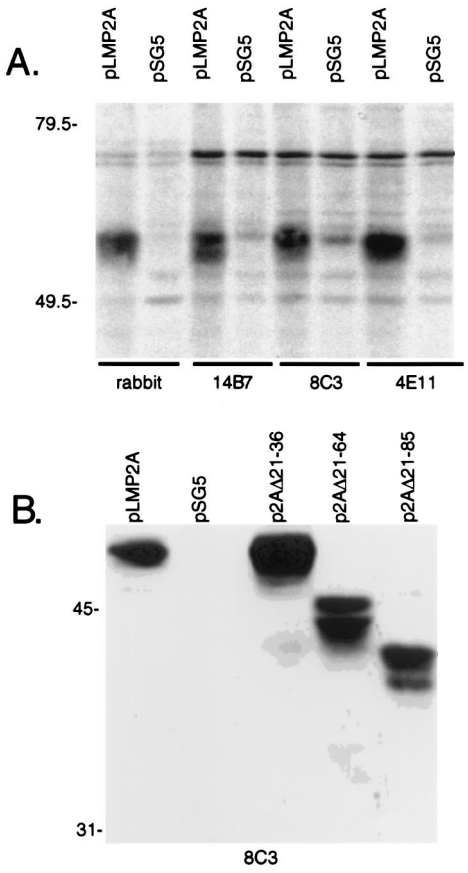

FIG. 4. Reactivity of the rat monoclonal antibodies with BJAB cells transfected with LMP2A expression constructs. (A) Immunoprecipitation of LMP2A from BJAB cells expressing wild-type LMP2A. For each immunoprecipitation, 10^7 BJAB cells were transfected with 50 μg of pLMP2A or vector alone (pSG5) and labeled with [^{35}S]methionine. Ten hours after transfection, cells were washed in PBS and lysed in 1% NP-40 lysis buffer and the insoluble material was removed by centrifugation at 4°C. Three rat monoclonal antibodies and rabbit polyclonal antisera were used to immunoprecipitate LMP2A from the transfected cells as described in Materials and Methods. (B) Reactivities of antibody 8C3 with wild-type and deletion mutant LMP2A protein in immunoblots of BJAB cells transfected with LMP2A cDNA expression constructs. NP-40-soluble lysates were prepared as described for panel A but were not immunoprecipitated. Lysates were separated by SDS–8% PAGE, transferred to nitrocellulose, probed with the rat monoclonal 8C3 antibody, incubated with HRP-linked secondary antibody, and detected by ECL. Approximately equivalent amounts of cellular proteins as determined by Ponceau S staining of the transferred proteins were loaded. Protein standards are indicated at the left in kilodaltons.

tions of LMP2A-expressing BJAB cells demonstrated reactivity with each of the three hybridoma supernatants which was not apparent in the control-transfected cells (Fig. 4A, lanes marked 14B7, 8C3, 4E11). A previously described rabbit polyclonal antiserum (20) was used as a positive control (Fig. 4A, lanes marked rabbit).

To determine which of the rat antibodies would recognize the three LMP2A deletion mutants, immunofluorescence was performed on BJAB cells transfected with LMP2A and LMP2A deletion mutations (Table 1). The results indicate that the presence of amino acids 21 to 36 was required for 4E11 reactivity, amino acids 36 to 64 were required for 14B7 reactivity, and amino acids 86 to 112 were required for 8C3 reactivity with LMP2A (Fig. 1C). To confirm these results, the hybridoma supernatants were used in immunoblots with BJAB cells transfected with LMP2A and LMP2A deletion mutant cDNA constructs corresponding to the LMP2A mutations that were recombined into the EBV genome. All three antibodies detected wild-type LMP2A protein in immunoblots (data not shown). Antibody 14B7 had the greatest sensitivity to LMP2A protein but was limited to detection of wild-type LMP2A and the LMP2AΔ21-36 deletion mutant (data not shown). 14B7 did not detect the larger two deletion mutants (LMP2AΔ21-64 and LMP2AΔ21-85 [data not shown]). Antibody 4E11 reacted with wild-type LMP2A protein in immunoblots but not with any of the three LMP2A deletion mutant proteins (data not shown). However, antibody 8C3 reacted with all three LMP2A deletion mutants (Fig. 4B) and was used to verify LMP2A expression in LCLs infected with each of the LMP2A deletion mutations.

LMP2A protein expression in EBV$^+$ LMP2A deletion mutant LCLs. Expression of LMP2A in EBV$^+$ LMP2A deletion mutant LCLs was confirmed in immunoblots with antibody 8C3, with representative data shown in Fig. 5. In a positive control, an EBV$^+$ LMP2A$^+$ LCL, wild-type LMP2A was clearly evident (Fig. 5, lane 1). For each of the EBV$^+$ LMP2A deletion mutant LCLs, LMP2A was detected and decreased in size, as expected, with each deletion (Fig. 5, lane 2, LMP2AΔ21-36 mutant; lane 3, LMP2AΔ21-64 mutant; and lane 4, LMP2AΔ21-85 mutant). Immunoblot analysis demonstrates that the deletion mutants express LMP2A at levels similar to those of EBV$^+$ LMP2A$^+$ LCLs (Fig. 5) and are of the expected sizes.

To verify that the subcellular localizations of the mutant

TABLE 1. Reactivity of rat monoclonal antibodies with LMP2A and LMP2A deletion mutants by immunofluorescence microscopy[a]

Expression vector	Antibody[b]		
	8C3	14B7	4E11
pSG5[c]	−	−	−
pLMP2A[c]	+	+	+
pLMP2B[c]	−	−	−
p2AΔ21-36[d]	+	+	−
p2AΔ21-64[d]	+	−	−
p2AΔ21-85[d]	+	−	−
p2AΔ85-112[d]	−	+	+
p2AΔ168-365[c]	+	+	+
p2AΔ168-497[c]	+	+	+
p2AΔ312-497[c]	+	+	+

[a] BJAB cells were transfected with LMP2A expression constructs, and immunofluorescence microscopy was performed as detailed in Materials and Methods.
[b] Hybridoma supernatants from the three rat monoclonal antibodies used in the immunofluorescence studies.
[c] LMP2A expression constructs previously described (19).
[d] LMP2A expression constructs detailed in Materials and Methods.

LMP2A proteins resembled that of wild-type LMP2A, immunofluorescence microscopy of EBV$^+$ LMP2A$^+$ and EBV$^+$ LMP2A deletion mutant LCLs was done (Fig. 6). There was no reactivity of the 8C3 antibody in the EBV-negative B-lymphoma cell line, BJAB (Fig. 6A). In contrast, panels C and E depict the bright, speckled fluorescence of LCLs expressing wild-type LMP2A and panels B, D, and F show the fluorescence of the LMP2AΔ21-36-, LMP2AΔ21-64-, and LMP2AΔ21-85-expressing LCLs. All three deletion mutants demonstrate the same bright, speckled fluorescence found in the EBV$^+$ LMP2A$^+$ LCLs. The immunofluorescence data demonstrate the similar subcellular localizations of LMP2A proteins in EBV$^+$ LMP2A$^+$ and EBV$^+$ LMP2A deletion mutant LCLs.

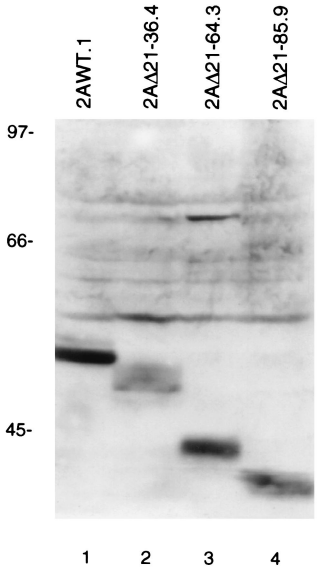

FIG. 5. Immunoblots with anti-LMP2A antibody 8C3 in wild-type and mutant EBV-infected LCLs. LCLs (10^7) were washed in PBS and lysed in 1% NP-40 lysis buffer, and the insoluble materials were removed by centrifugation at 4°C. The prepared lysates were separated by SDS–8% PAGE, transferred to nitrocellulose, probed with 8C3 antibody, incubated with HRP-linked secondary antibody, and detected by ECL. Approximately equivalent amounts of cellular proteins as determined by Ponceau S staining of the transferred proteins were loaded. Lane 1 demonstrates the wild-type LMP2A size, lane 2 shows the 16-amino-acid-smaller LMP2A of a representative LMP2AΔ21-36 mutant, lane 3 shows the 44-amino-acid-smaller LMP2A of an LMP2AΔ21-64 mutant, and lane 4 shows the 65-amino-acid-smaller LMP2A of an LMP2AΔ21-85 mutant LCL. Protein standards are indicated at the left in kilodaltons.

Induction of tyrosine phosphorylation in EBV$^+$ LMP2A$^+$ and EBV$^+$ LMP2A deletion mutant LCLs following sIg cross-linking. To assess the effects of the LMP2A deletion mutations on the dominant-negative effect of LMP2A on tyrosine phosphorylation following sIg cross-linking, EBV$^+$ LMP2A$^+$ and EBV$^+$ LMP2A deletion mutant LCLs, matched for sIg expression by flow cytometry (data not shown), were analyzed for induction of tyrosine phosphorylation following sIg cross-linking. Representative data are shown in two different exposures of the same immunoblot in Fig. 7A and B. In a representative EBV$^+$ LMP2A$^+$ LCL (Fig. 7, lanes 1 to 3), a number of proteins were constitutively phosphorylated in unstimulated LCLs (Fig. 7A, lane 1) and this pattern remained relatively unchanged after sIg cross-linking (Fig. 7A, lanes 2 and 3), except that a protein of approximately 70 kDa exhibited some induction of tyrosine phosphorylation. This resembles a previously reported circumstance (28). As also described earlier, LMP2A was the dominant phosphorylated protein in EBV$^+$ LMP2A$^+$ LCLs and its level of phosphorylation did not change over time (Fig. 7, lanes 1 to 3). This band was confirmed as LMP2A by stripping the blot and reprobing it with the antibody 8C3 (data not shown). There was an additional constitutively phosphorylated cellular protein that comigrated with LMP2A. Like EBV$^+$ LMP2A$^+$ LCLs, LMP2AΔ21-36 LCLs showed constitutive phosphorylation of the same proteins in untreated LCLs and slight induction of phosphorylation of the 70-kDa protein following sIg cross-linking (Fig. 7A, lanes 4 to 6). The smaller size of mutated LMP2AΔ21-36 is indicated by an arrow (Fig. 7, lanes 4 to 6) and confirmed by its reactivity with antibody 8C3 (data not shown). However, in LMP2AΔ21-64-infected LCLs, there was little constitutive phosphorylation in untreated cells (Fig. 7A, lane 7), but upon sIg cross-linking, there was a dramatic increase in the number of proteins which were tyrosine phosphorylated (Fig. 7A, lanes 7 to 9). This increase in tyrosine-phosphorylated proteins, following sIg cross-linking, was similar to what was observed in EBV$^+$ LMP2A$^-$ LCLs or in an EBV$^-$ B-lymphoma cell line (28). Interestingly, the mutant LMP2A protein was phosphorylated following cross-linking and not constitutively phosphorylated before sIg cross-linking (Fig. 7B, lanes 7 to 9). The identity of the mutant LMP2A protein was confirmed by immunoblot analysis (data not shown). In LMP2AΔ21-85 LCLs, proteins of approximately 65 and 60 kDa were constitutively phosphorylated in untreated cells (Fig. 7A, lane 10). These proteins are likely the same proteins which are constitutively phosphorylated in EBV$^+$ LMP2A$^+$ LCLs (Fig. 7A, lane 1). Following sIg cross-linking, there was an increase in tyrosine-phosphorylated proteins in the LMP2AΔ21-85 LCLs, but their appearance was somewhat delayed when compared with that of the LMP2AΔ21-64-infected LCLs (Fig. 7A) or EBV$^+$ LMP2A$^-$ LCLs as previously published (28). The LMP2AΔ21-85 protein was not detected when the blot was stripped and reprobed with 8C3 antibody, indicating that the mutant LMP2A protein was not highly tyrosine phosphorylated in LMP2AΔ21-85-infected LCLs (Fig. 7B, lanes 10 to 12).

Calcium mobilization in EBV$^+$ LMP2A$^+$ and EBV$^+$ LMP2A deletion mutant LCLs following sIg cross-linking. Previous experiments had determined that LMP2A blocked normal calcium mobilization following sIg cross-linking both in EBV$^-$ B-lymphoma cell lines expressing LMP2A and in EBV$^+$ LMP2A$^+$ LCLs (29, 30). Calcium mobilization was not

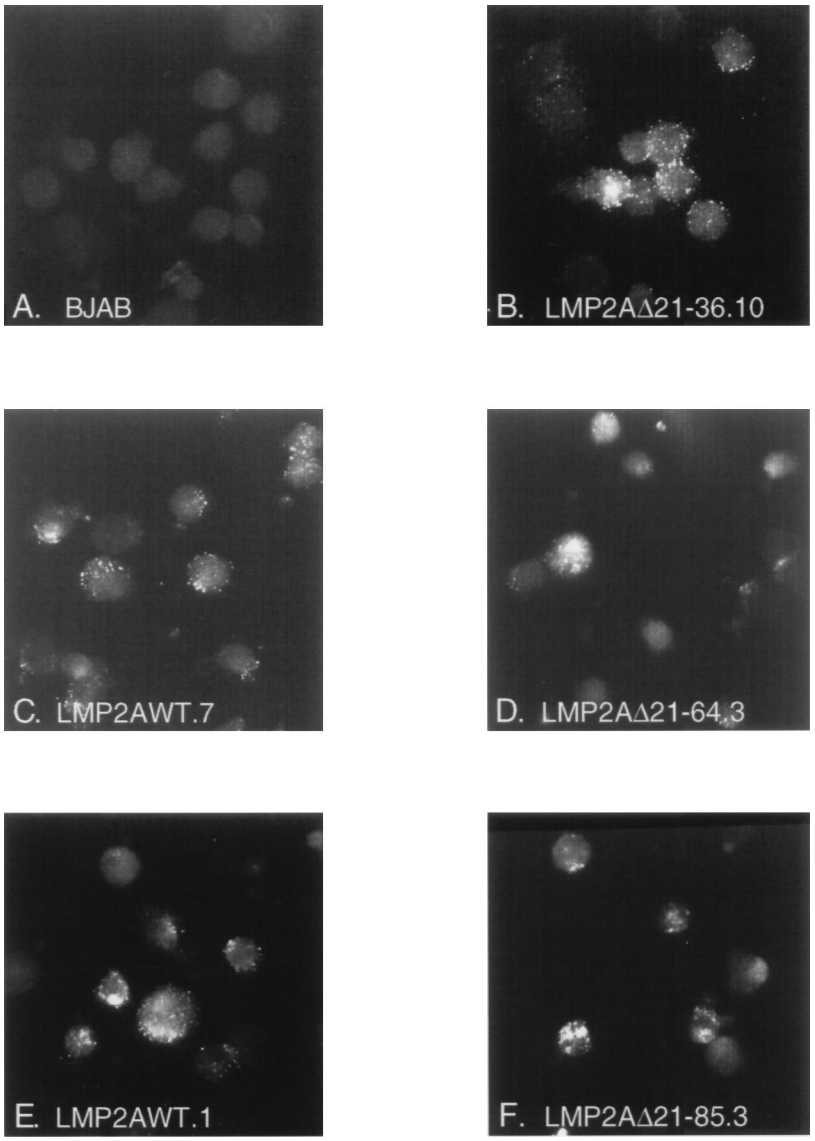

FIG. 6. Immunofluorescence microscopy of wild-type and LMP2A mutant EBV-infected LCLs with antibody 8C3. LCLs were fixed to glass slides, incubated with 8C3, and reacted with a tetramethyl rhodamine isothiocyanate-labeled secondary antibody. (A) Dull, background fluorescence of the EBV$^-$ cell line BJAB. Panels C and E depict the bright, speckled fluorescence of LCLs expressing wild-type LMP2A. Panels B, D, and F show the fluorescence of the LMP2AΔ21-36-, LMP2AΔ21-64-, and LMP2AΔ21-85-expressing LCLs. All three deletion mutants demonstrate the same bright, speckled fluorescence as in the wild-type LMP2A-expressing LCLs.

blocked in EBV$^+$ LMP2A$^-$ LCLs (29). To assess the effects of the LMP2A deletion mutants on calcium mobilization, multiple EBV$^+$ LMP2A$^+$ and EBV$^+$ LMP2A deletion mutant LCLs derived in parallel and matched for sIg expression by flow cytometry (data not shown) were loaded with the calcium-binding dye fluo-3 and monitored for fluorescence after sIg cross-linking. Previously described EBV$^+$ LMP2A$^+$ (Table 2; WT1 and WT4) and EBV$^+$ LMP2A$^-$ (Table 2; ES1 and ES2) LCLs were included as controls (29). EBV$^+$ LMP2A$^+$ LCLs demonstrated a minimal calcium flux after treatment with sIg (8 to 40%) (Table 2). These calcium flux values appear negligible when compared with the calcium flux values of the EBV$^+$ LMP2A$^-$ LCLs (8 to 40% versus 231 to 244%, respectively) (Table 2). Representative EBV$^+$ LMP2A deletion mutant LCLs were also tested. These data indicate that both the LMP2AΔ21-36 and LMP2AΔ21-64 deletion mutants have calcium flux phenotypes similar to those of EBV$^+$ LMP2A$^+$ LCLs (Table 2). Representative LMP2AΔ21-85 mutants had an observed mean calcium flux of 49 to 118% (Table 2), a mean greater than EBV$^+$ LMP2A$^+$ LCLs (8 to 40%) but not as high as the mean calcium flux for the EBV$^+$ LMP2A$^-$ LCLs (231 to 244%).

Induction of EBV lytic replication in LMP2AΔ21-64 and LMP2AΔ21-85 LCLs following sIg cross-linking. Previous experiments demonstrated that activation of lytic replication was blocked in EBV$^+$ LMP2A$^+$ LCLs following sIg cross-linking but not in EBV$^+$ LMP2A$^-$ LCLs (29). Since calcium mobilization and induction of tyrosine phosphorylation following sIg cross-linking were altered in LMP2AΔ21-64 and LMP2AΔ21-85 LCLs unlike with EBV$^+$ LMP2A$^+$ LCLs, activation of lytic replication in LMP2AΔ21-64 and LMP2AΔ21-85 LCLs was investigated following sIg cross-linking. Representative LCLs infected with each mutation were either untreated or treated with goat anti-human Ig for 48 h and monitored for

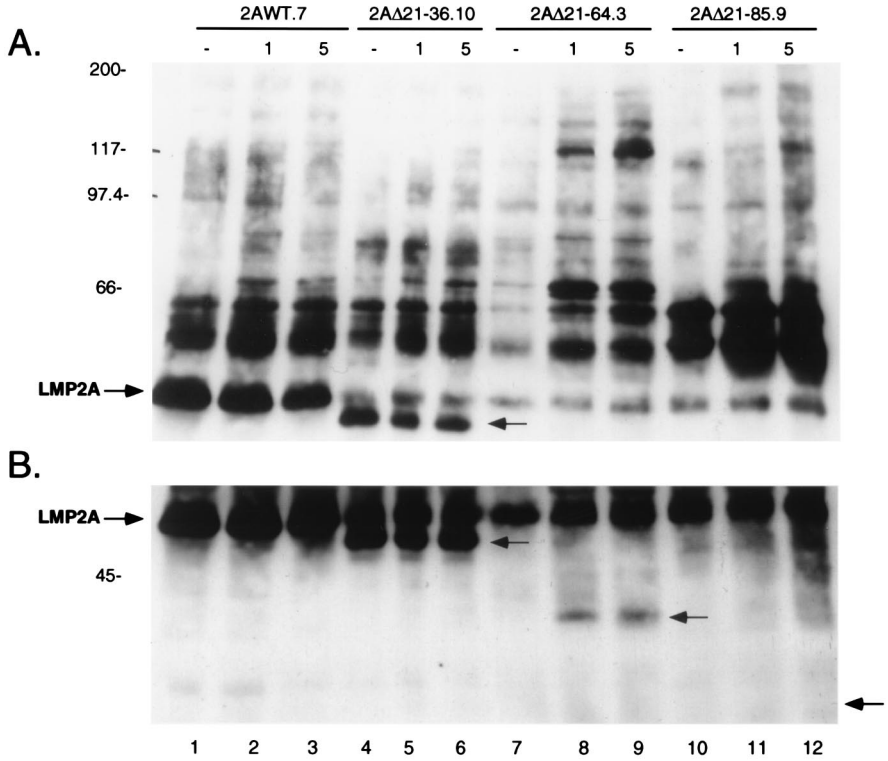

FIG. 7. Tyrosine phosphorylation following sIg cross-linking of wild-type and mutant LMP2A-expressing EBV-infected LCLs. (A and B) Two different exposures of the same immunoblot. The positions of LMP2A are noted with arrows. Cells were either untreated (minus) or treated at 2×10^7 cells per ml with anti-Ig antibody for the indicated times (1 and 5 min) and lysed in 1% NP-40 lysis buffer. Insoluble materials were removed by centrifugation at 4°C, and cleared lysates were immunoprecipitated with PY20 antiphosphotyrosine antibody and captured with protein A-Sepharose beads. Captured lysates were washed in lysis buffer and separated by SDS–8% PAGE. The fractionated proteins were transferred to nitrocellulose, immunoblotted with the HRP-coupled PY20 antibody, washed in TBST, and detected by ECL. Approximately equivalent amounts of cellular proteins as determined by Ponceau S staining of the transferred proteins were loaded. Protein standards are indicated at the left in kilodaltons.

anti-Ig-induced expression of Z, the BZLF1 immediate-early gene product, by immunoblotting with monoclonal BZ1 antibody or with a human serum reactive to EBV lytic antigens (29, 49). In three of four different LMP2AΔ21-64 LCLs, lytic replication was readily induced following sIg cross-linking (data not shown). Two LCLs (LMP2AΔ21-64.1 and -64.6) were tested in four individual experiments to confirm the reproducibility of the results, while two LCLs (LMP2AΔ21-64.3 and -64.5) were tested only once. In two different LMP2AΔ21-85 LCLs, lytic replication was never induced following sIg cross-linking (data not shown). One LCL (LMP2AΔ21-85.9) was tested four times, and the other LCL (LMP2AΔ21-85.3) was tested two times with reproducible results. Previously described EBV^+ $LMP2A^+$ and EBV^+ $LMP2A^-$ LCLs (WT1 and ES1) were included as controls and behaved as expected. These data indicate that LMP2AΔ21-64 LCLs are phenotypically similar to EBV^+ $LMP2A^-$ LCLs, while LMP2Δ21-85 LCLs are similar to EBV^+ $LMP2A^+$ LCLs in regard to activation of lytic replication following sIg cross-linking.

DISCUSSION

Three deletion mutations of LMP2A have been recombined into the EBV genome and verified by both PCR and Southern blot analysis. The mutations do not alter the level of expression or subcellular localization of LMP2A in EBV-infected LCLs. The first LMP2A deletion mutation, LMP2AΔ21-36, deletes 16 amino acids, including Y-23 and Y-31. LCLs transformed with EBV containing this mutation behaved like EBV^+ $LMP2A^+$ LCLs, fully able to prevent sIg cross-linking-induced tyrosine phosphorylation and calcium mobilization. Interestingly, Y-23 is changed to a glycine in the LMP2A of herpesvirus papio (7) and changed to an aspartic acid in 28 clinical EBV isolates which have been sequenced (3) and does not contain a sequence motif that would predict binding to an identified SH2 domain. Y-31, although within a sequence motif that could bind group III SH2 members (40, 41), appears, along with Y-23, not to be essential for LMP2A's dominant-negative effect on sIg-mediated signal transduction.

The second LMP2A deletion mutation, LMP2AΔ21-64, deletes 44 amino acids, including Y-23, Y-31, Y-60, Y-64, and one of the two PY motifs (6, 43) in the amino-terminal domain of LMP2A that could mediate the binding of proteins with a WW domain (6, 43). The Y-60 and Y-64 sequence motifs are conserved in LMP2A of herpesvirus papio, although there are an additional six amino acids between the motifs in herpesvirus papio (7). However, in the sequenced clinical EBV isolates, most of which are from EBV-related malignancies, Y-64 was changed to aspartic acid in roughly half of the isolates (3) while Y-60 was conserved in all of the isolates (3). Like EBV^+ $LMP2A^+$ LCLs, the LMP2AΔ21-64 LCLs demonstrated little change in intracellular calcium concentrations following sIg cross-linking. Interestingly, the extent of induction of tyrosine phosphorylation and the activation to lytic replication after sIg cross-linking displayed by these same mutant LCLs resembled that of EBV^+ $LMP2A^-$ LCLs. The third LMP2A deletion mutation, LMP2AΔ21-85, deletes 65 amino acids, including

TABLE 2. Calcium flux of wild-type and recombinant LMP2A LCLs after sIg cross-linking[a]

Cell line type and name[b]	No.[c]	% Calcium increase[d]
EBV$^+$ LMP2A$^+$ LCLs		
WT1	7	8 (0–21)
WT4	11	13 (0–31)
LMP2AWT.1	3	40 (0–65)
LMP2AWT.2	2	13 (11–13)
LMP2AWT.6	3	16 (10–22)
LMP2AWT.7	3	26 (12–51)
LMP2AWT.3.7	3	17 (15–19)
LMP2AWT.23	3	18 (9–23)
EBV$^+$ LMP2A$^-$ LCLs		
ES1	5	244 (131–423)
ES4	13	231 (131–345)
EBV$^+$ LMP2A deletion mutant LCLs		
LMP2AΔ21-36.4	1	24
LMP2AΔ21-36.8	1	37
LMP2AΔ21-36.10	3	18 (10–31)
LMP2AΔ21-36.1	3	30 (29–30)
LMP2AΔ21-36.G.4	3	57 (43–67)
LMP2AΔ21-36.2	3	36 (25–44)
LMP2AΔ21-64.1	4	15 (3–24)
LMP2AΔ21-64.3	5	23 (0–41)
LMP2AΔ21-64.5	3	19 (17–22)
LMP2AΔ21-64.6	4	16 (10–22)
LMP2AΔ21-85.3	5	49 (32–71)
LMP2AΔ21-85.9	3	118 (89–161)

[a] LCLs (3×10^6 cells) were resuspended in loading buffer and loaded with 2 mM fluo-3 for 30 min at RT. Following loading, LCLs were washed twice and resuspended in loading buffer. The prepared cells were then measured for fluorescence after sIg cross-linking in a Perkin-Elmer LS-5B luminescence spectrometer. The excitation and emission values for fluo-3 were 505 and 530 nm, respectively. The autofluorescence (or minimal fluorescence) for each LCL was also determined by performing the above procedure without adding the fluo-3 dye. The baseline fluorescence was recorded for 1 min, and the maximal fluorescence was measured after the addition of digitonin. Calcium concentrations were calculated according to the formula $Ca^{2+} = 400(F - \text{Fmin})/(\text{Fmax} - F)$, where F is baseline fluorescence, Fmin is minimal fluorescence, and Fmax is maximal fluorescence (18, 27).

[b] WT1, WT4, ES1, and ES4 were previously described LCLs (29). All other LCLs were produced in this study.

[c] Number of times calcium mobilization was determined for each LCL.

[d] The mean percent increase of calcium was calculated for each LCL. Values in parentheses are the ranges in percent calcium increase determined for each LCL that were used to calculate the mean percent calcium increases.

Y-74 and Y-85, that are homologous to the ITAM motif, not changed in any EBV clinical isolates sequenced to date (3), and found within a highly conserved region of the herpesvirus papio LMP2A (7). This strong conservation implies this region of LMP2A may be important for LMP2A function. LMP2AΔ21-85 LCLs do not behave like EBV$^+$ LMP2A$^-$ LCLs, or like EBV$^+$ LMP2A$^+$ LCLs. Rather, they exhibit constitutive phosphorylation of the 60- and 65-kDa proteins (resembling that observed in unstimulated EBV$^+$ LMP2A$^+$ LCLs), a delay in induction of tyrosine phosphorylation following sIg cross-linking, and intermediate calcium mobilization when compared with EBV$^+$ LMP2A$^+$ LCLs and EBV$^+$ LMP2A$^-$ LCLs. Like EBV$^+$ LMP2A$^+$ LCLs, lytic replication is not activated following sIg cross-linking.

The experimental results with LMP2AΔ21-64 LCLs and LMP2AΔ21-85 LCLs in regard to calcium mobilization, induction of tyrosine phosphorylation, and activation of lytic replication are incongruous. In regard to induction of tyrosine phosphorylation and activation of lytic replication, LMP2AΔ21-64 LCLs behave like EBV$^+$ LMP2A$^-$ LCLs while LMP2AΔ21-85 LCLs have a delayed induction of tyrosine phosphorylation and no activation of lytic replication. In calcium mobilization experiments, LMP2AΔ21-64 LCLs behave like EBV$^+$ LMP2A$^+$ LCLs while LMP2AΔ21-85 LCLs have an intermediate calcium mobilization phenotype. The Y-64 motif is not predicted to bind any known SH2 domain, while Y-60 has the best homology with motifs which bind the Nck SH2 domain or other adaptor proteins. Adaptor proteins are important in coupling membrane-proximal signaling events with downstream events (34, 35), but there is no evidence to suggest they have a role in the induction of tyrosine phosphorylation following receptor activation. Therefore, it is somewhat surprising that a mutation in this LMP2A domain restores normal induction of tyrosine phosphorylation following sIg cross-linking. From predicted specificities of known SH2 domains, Y-60 would not appear to bind PTKs. Of the two PTKs known to bind LMP2A, Y-74 and Y-85 have the best homology to the Syk PTK SH2 domain preferred binding motif, and Y-112 has the best homology to the Src family PTK SH2 domain binding motif. Although unlikely, LMP2A may alter the activity of a protein involved in regulation of tyrosine phosphorylation following sIg cross-linking; the portion of LMP2A mediating this effect may be deleted in the LMP2AΔ21-64 LCLs. Possible protein targets affected by LMP2A include other PTKs, phosphatases, regulators of the Src family or Syk PTKs, or WW domain-containing proteins.

A more plausible explanation of the LMP2AΔ21-64 mutant phenotype is based on the observation that LMP2A is not constitutively phosphorylated in LMP2AΔ21-64 LCLs but becomes phosphorylated following sIg cross-linking. Since LMP2A is not constitutively phosphorylated, downstream effector molecules may not load onto the LMP2A receptor tail-like domains and be negatively regulated. However, once LMP2A becomes phosphorylated upon sIg cross-linking, effector molecules, important for calcium mobilization, load onto the mutant LMP2A and their activities are down-modulated. This effect on LMP2A function may be the result of structural alterations in LMP2A that lead to inefficient tyrosine phosphorylation of LMP2A tyrosines prior to PTK activation.

The LMP2AΔ21-85 mutant form of LMP2A clearly has more wild-type activity than the LMP2AΔ21-64 mutation. Like EBV$^+$ LMP2A$^+$ LCLs, the constitutive phosphorylation of the 65- and 60-kDa proteins is observed in LMP2AΔ21-85 LCLs but not in LMP2AΔ21-64 LCLs. In addition, there is only a partial block in signal transduction as measured by induction of tyrosine phosphorylation and calcium mobilization. In this regard, LMP2AΔ21-85 LCLs are similar to Lyn-deficient chicken B cells, which demonstrate delayed tyrosine phosphorylation and calcium mobilization following sIg cross-linking (45). Syk-deficient chicken B cells also demonstrate delayed tyrosine phosphorylation but are unable to mobilize calcium (45). Therefore, it seems likely that Lyn activity but not Syk activity is affected in the LMP2AΔ21-85 LCLs. The absence of a similar effect in the LMP2AΔ21-64 LCLs may be due to improper folding of the LMP2AΔ21-64 protein, resulting in an inactive LMP2A protein which is not optimally recognized by effector molecules. Further site-specific mutations of this LMP2A region will delineate between these possibilities.

It is hypothesized that LMP2A mimics cross-linked cell surface receptors, resulting in the recruitment of cellular PTKs and other proteins involved in signal transduction and thereby leading to down-modulation of their activity. Certain regions of LMP2A, as shown in this study, are vital for LMP2A function, while others appear dispensable. LMP2A function is likely important in preventing the activation of lytic viral infection in EBV-infected B lymphocytes as they traffic through

the peripheral blood, lymphatic tissue, or bone marrow where B-cell activation would activate lytic viral replication. Further delineation of LMP2A domains important for LMP2A function and cellular proteins whose activities are modulated by LMP2A will aid in the study of herpesvirus latency and may provide insight into how latent infections in humans can be controlled or eradicated.

ACKNOWLEDGMENTS

We are grateful for Elliott Kieff's continued support. We thank Cheryl Miller for providing invaluable aid and Lawrence Young for the BZ1 monoclonal antibody. We thank Nikolaus Mueller-Lantzsch and Georg Bornkamm, who initiated the production of the monoclonal antibodies, for aid and helpful discussions.

This research was supported by Public Health Service grants CA62234 (R.L.) from the National Cancer Institute. R.L. is a scholar of the Leukemia Society of America. N. Mueller-Lantzsch was supported by a grant from the Deutsche Krebshilfe (W96/94/Mü2 and W4791/Mü1), and G. Laux was supported by grants Fa138/3-4 and Fa138/3-7 from the Deutsche Forschungsgemeinschaft.

REFERENCES

1. **Bolen, J. B.** 1993. Nonreceptor tyrosine protein kinases. Oncogene **8:**2025–2031.
2. **Burkhardt, A. L., J. B. Bolen, E. Kieff, and R. Longnecker.** 1992. An Epstein-Barr virus transformation-associated membrane protein interacts with *src* family tyrosine kinases. J. Virol. **66:**5161–5167.
3. **Busson, P., R. H. Edwards, T. Tursz, and N. Raab-Traub.** 1995. Sequence polymorphism in the Epstein-Barr virus latent membrane protein (LMP)-2 gene. J. Gen. Virol. **76:**139–145.
4. **Cambier, J. C.** 1995. New nomenclature for the Reth motif (or ARH1/TAM/ARAM/YXXL). Immunol. Today **16:**110.
5. **Cambier, J. C., C. M. Pleiman, and M. R. Clark.** 1994. Signal transduction by the B cell antigen receptor and its coreceptors. Annu. Rev. Immunol. **12:**457–486.
6. **Chen, H. I., and M. Sudol.** 1995. The WW domain of Yes-associated protein binds a proline-rich ligand that differs from the consensus established for Src homology 3-binding modules. Proc. Natl. Acad. Sci. USA **92:**7819–7823.
7. **Franken, M., B. Annis, A. N. Ali, and F. Wang.** 1995. 5′ coding and regulatory region sequence divergence with conserved function of the Epstein-Barr virus LMP2A homolog in herpesvirus papio. J. Virol. **69:**8011–8019.
8. **Frech, B., U. Zimber-Strobl, K. O. Suentzenich, O. Pavlish, G. M. Lenoir, G. W. Bornkamm, and N. Mueller-Lantzsch.** 1990. Identification of Epstein-Barr virus terminal protein 1 (TP1) in extracts of four lymphoid cell lines, expression in insect cells, and detection of antibodies in human sera. J. Virol. **64:**2759–2767.
9. **Frech, B., U. Zimber-Strobl, T. T. Yip, W. H. Lau, and N. Mueller-Lantzsch.** 1993. Characterization of the antibody response to the latent infection terminal proteins of Epstein-Barr virus in patients with nasopharyngeal carcinoma. J. Gen. Virol. **74:**811–818.
10. **Heston, L., M. Rabson, N. Brown, and G. Miller.** 1982. New Epstein-Barr virus variants from cellular subclones of P3J-HR-1 Burkitt lymphoma. Nature (London) **295:**160–163.
11. **Kieff, E.** 1996. Epstein-Barr virus and its replication, p. 1109–1162. *In* B. N. Fields, D. M. Knipe, P. M. Howley, et al. (ed.), Fundamental virology. Raven Press, New York.
12. **Kieff, E., and D. Liebowitz.** 1990. Epstein-Barr virus and its replication, p. 1889–1920. *In* B. N. Fields and D. M. Knipe (ed.), Virology. Raven Press, New York.
13. **Kim, O. J., and J. L. Yates.** 1993. Mutants of Epstein-Barr virus with a selective marker disrupting the TP gene transform B cells and replicate normally in culture. J. Virol. **67:**7634–7640.
14. **Koerner, T. J., J. E. Hill, A. M. Myers, and A. Tzagoloff.** 1991. High-expression vectors with multiple cloning sites for construction of trpE fusion genes: pATH vectors. Methods Enzymol. **194:**477–490.
15. **Kremmer, E., B. R. Kranz, A. Hille, K. Klein, M. Eulitz, G. Hoffmann-Fezer, W. Feiden, K. Herrmann, H.-J. Delecluse, G. Delsol, G. W. Bornkamm, N. Mueller-Lantzsch, and F. A. Grässer.** 1995. Rat monoclonal antibodies differentiating between the Epstein-Barr virus nuclear antigens 2A (EBNA2A) and 2B (EBNA2B). Virology **208:**336–342.
16. **Laux, G., A. Economou, and P. J. Farrell.** 1989. The terminal protein gene 2 of Epstein-Barr virus is transcribed from a bidirectional latent promoter region. J. Gen. Virol. **70:**3079–3084.
17. **Laux, G., M. Perricaudet, and P. J. Farrell.** 1988. A spliced Epstein-Barr virus gene expressed in immortalized lymphocytes is created by circularization of the linear viral genome. EMBO J. **7:**769–774.
18. **Lee, S. K., and P. H. Stern.** 1994. Studies on the mechanism of desensitization of the parathyroid hormone-stimulated calcium signal in UMR-106 cells: reversal of desensitization by alkaline phosphatase but not by protein kinase C downregulation. J. Bone Miner. Res. **9:**781–789.
19. **Longnecker, R., B. Druker, T. M. Roberts, and E. Kieff.** 1991. An Epstein-Barr virus protein associated with cell growth transformation interacts with a tyrosine kinase. J. Virol. **65:**3681–3692.
20. **Longnecker, R., and E. Kieff.** 1990. A second Epstein-Barr virus membrane protein (LMP2) is expressed in latent infection and colocalizes with LMP1. J. Virol. **64:**2319–2326.
21. **Longnecker, R., and C. L. Miller.** 1996. Regulation of Epstein-Barr virus latency by latent membrane protein 2. Trends Microbiol. **4:**38–42.
22. **Longnecker, R., C. L. Miller, X-Q. Miao, A. Marchini, and E. Kieff.** 1992. The only domain which distinguishes Epstein-Barr virus latent membrane 2A (LMP2A) from LMP2B is dispensable for lymphocyte infection and growth transformation in vitro, and LMP2A is therefore nonessential. J. Virol. **66:**6461–6469.
23. **Longnecker, R., C. L. Miller, X-Q. Miao, B. Tomkinson, and E. Kieff.** 1993. The last seven transmembrane and carboxy-terminal cytoplasmic domains of Epstein-Barr virus latent membrane 2 (LMP2) are dispensable for lymphocyte infection and growth transformation in vitro. J. Virol. **67:**2006–2013.
24. **Longnecker, R., C. L. Miller, B. Tomkinson, X-Q. Miao, and E. Kieff.** 1993. Deletion of DNA encoding the first five transmembrane domains of Epstein-Barr virus latent membrane proteins 2A and 2B. J. Virol. **67:**5068–5074.
25. **Marchini, A., B. Tomkinson, J. I. Cohen, and E. Kieff.** 1991. BHRF1, the Epstein-Barr virus gene with homology to Bc12, is dispensable for B-lymphocyte transformation and virus replication. J. Virol. **65:**5991–6000.
26. **Menezes, J., W. Leibold, G. Klein, and G. Clements.** 1975. Establishment and characterization of an Epstein-Barr virus (EBV)-negative lymphoblastoid B cell line (BJA-B) from an exceptional, EBV-genome-negative African Burkitt's lymphoma. Biomedicine **22:**276–284.
27. **Merrit, J. E., S. A. McCarthy, M. P. A. Davies, and K. E. Moores.** 1990. Use of fluo-3 to measure cytosolic Ca2+ in platelets and neutrophils. Biochem. J. **269:**513–519.
28. **Miller, C. L., A. L. Burkhardt, J. H. Lee, B. Stealey, R. Longnecker, J. B. Bolen, and E. Kieff.** 1995. Integral membrane protein 2 of Epstein-Barr virus regulates reactivation from latency through dominant negative effects on protein-tyrosine kinases. Immunity **2:**155–166.
29. **Miller, C. L., J. H. Lee, E. Kieff, and R. Longnecker.** 1994. An integral membrane protein (LMP2) blocks reactivation of Epstein-Barr virus from latency following surface immunoglobulin crosslinking. Proc. Natl. Acad. Sci. USA **91:**772–776.
30. **Miller, C. L., R. Longnecker, and E. Kieff.** 1993. Epstein-Barr virus latent membrane protein 2A blocks calcium mobilization in B lymphocytes. J. Virol. **67:**3087–3094.
31. **Miller, G.** 1990. The Epstein-Barr virus, p. 563–589. *In* B. N. Fields and D. M. Knipe (ed.), Virology. Raven Press, New York.
32. **Miller, G., and M. Lipman.** 1973. Release of infectious Epstein-Barr virus by transformed marmoset leukocytes. Proc. Natl. Acad. Sci. USA **70:**190–194.
33. **Miller, G., T. Shope, H. Lisco, D. Stitt, and M. Lipman.** 1972. Epstein-Barr virus: transformation, cytopathic changes, and viral antigens in squirrel monkey and marmoset leukocytes. Proc. Natl. Acad. Sci. USA **69:**383–387.
34. **Pawson, T.** 1993. Signal transduction—a conserved pathway from the membrane to the nucleus. Dev. Genet. **14:**333–338.
35. **Pawson, T., P. Olivier, A. M. Rozakis, J. McGlade, and M. Henkemeyer.** 1993. Proteins with SH2 and SH3 domains couple receptor tyrosine kinases to intracellular signalling pathways. Philos. Trans. R. Soc. Lond. B **340:**279–285.
36. **Qu, L., and D. Rowe.** 1992. Epstein-Barr virus latent gene expression in uncultured peripheral blood lymphocytes. J. Virol. **66:**3715–3724.
37. **Reth, M.** 1989. Antigen receptor tail clue. Nature (London) **338:**383–384.
38. **Rowe, D. T., L. Hall, I. Joab, and G. Laux.** 1990. Identification of the Epstein-Barr virus terminal protein gene products in latently infected lymphocytes. J. Virol. **64:**2866–2875.
39. **Sample, J., D. Liebowitz, and E. Kieff.** 1989. Two related Epstein-Barr virus membrane proteins are encoded by separate genes. J. Virol. **63:**933–937.
40. **Songyang, Z., S. E. Shoelson, M. Chaudhuri, G. Gish, T. Pawson, W. G. Haser, F. King, T. Roberts, S. Ratnofsky, R. J. Lechleider, et al.** 1993. SH2 domains recognize specific phosphopeptide sequences. Cell **72:**767–778.
41. **Songyang, Z., S. E. Shoelson, J. McGlade, P. Olivier, T. Pawson, X. R. Bustelo, M. Barbacid, H. Sabe, H. Hanafusa, T. Yi, R. Ren, D. Baltimore, S. Ratinofsky, R. A. Feldman, and L. C. Cantley.** 1994. Specific motifs recognized by the SH2 domains of Csk, 3BP2, fps/fes, GRB-2, HCP, SHC, Syk, and Vav. Mol. Cell. Biol. **14:**2777–2785.
42. **Springer, T. A., A. Bhattacharya, J. T. Cardoza, and F. Sanchez-Madrid.** 1982. Monoclonal antibodies specific for rat IgG1, IgG2a, and IgG2b subclasses, and kappa chain monotypic and allotypic determinants: reagents for use with rat monoclonal antibodies. Hybridoma **1:**257–273.
43. **Sudol, M., P. Bork, A. Einbond, K. Kastury, T. Druck, M. Negrini, K. Hueber, and D. Lehman.** 1995. Characterization of the mammalian YAP (Yes-associated protein) gene and its role in defining a novel protein module, the WW domain. J. Biol. Chem. **270:**14733–14741.

44. **Swaminathan, S., B. Tomkinson, and E. Kieff.** 1991. Recombinant Epstein-Barr virus with small RNA (EBER) genes deleted transforms lymphocytes and replicates in vitro. Proc. Natl. Acad. Sci. USA **88:**1546–1550.
45. **Takata, M., H. Sabe, A. Hata, T. Inazu, Y. Homma, T. Nukada, H. Yamamura, and T. Kurosaki.** 1994. Tyrosine kinases Lyn and Syk regulate B cell receptor-coupled Ca2+ mobilization through distinct pathways. EMBO J. **13:**1341–1349.
46. **Tierney, R. J., N. Steven, L. S. Young, and A. B. Rickinson.** 1994. Epstein-Barr virus latency in blood mononuclear cells: analysis of viral gene transcription during primary infection and in the carrier state. J. Virol. **68:**7374–7385.
47. **Wang, F., A. Marchini, and E. Kieff.** 1991. Epstein-Barr virus (EBV) recombinants: use of positive selection markers to rescue mutants in EBV-negative B-lymphoma cells. J. Virol. **65:**1701–1709.
48. **Weiss, A., and D. R. Littman.** 1994. Signal transduction by lymphocyte antigen receptors. Cell **76:**263–274.
49. **Young, L. S., R. Lau, M. Rowe, G. Niedobitek, G. Packham, F. Shanahan, D. T. Rowe, D. Greenspan, J. S. Greenspan, A. B. Rickinson, and P. J. Farrell.** 1991. Differentiation-associated expression of the Epstein-Barr virus BZLF1 transactivator protein in oral hairy leukoplakia. J. Virol. **65:**2868–2874.